Hindawi
International Transactions on Electrical Energy Systems
Volume 2023, Article ID 4930801, 12 pages
https://doi.org/10.1155/2023/4930801

Research Article

Distribution of Currents in 2 × 25 kV Electric Railway Systems under Normal Conditions

Elmer Sorrentino,[1,2] **Naren Gupta**,[3] **Miguel Montilla-DJesus**,[2] **and Pablo Arriaga**[4]

[1]*Universidad Simón Bolívar, Caracas, Venezuela*
[2]*Universidad Carlos III de Madrid, Madrid, Spain*
[3]*Edinburgh Napier University, Edinburgh, UK*
[4]*Siemens, Caracas, Venezuela*

Correspondence should be addressed to Elmer Sorrentino; elmer.sorrentino@uc3m.es

Received 17 September 2022; Revised 20 January 2023; Accepted 24 January 2023; Published 8 February 2023

Academic Editor: C. Dhanamjayulu

This article shows a detailed analysis of the distribution of currents in 2 × 25 kV electric railway systems under normal conditions. The network equations are clearly formulated in a way that enables the presentation of a novel simplified analytical solution as well as the traditional numerical solution of the equation set. The simplified analytical solution is obtained when the transformer impedances are neglected, and under these conditions: (a) the distributions of currents are analytically deduced for cases with only one train; (b) the distribution of currents among autotransformers and between catenary and feeder can be easily understood, as well as the effect of the train position on the distribution of currents; and (c) the superposition method is applied for cases with multiple trains in order to clearly explain the distribution of currents from the results with only one train. On the other hand, the network equations are also numerically solved, including autotransformer impedances, and it is shown that their effect is very low, especially because these impedances are typically small. Therefore, the proposed analytical method is a good tool to obtain an easy and approximate solution for the distribution of currents in these systems, as well as an excellent tool to facilitate the understanding of that distribution.

1. Introduction

There are different electric railway systems; some of them are fed in DC, whereas others are fed in AC, and different voltage levels are currently applied around the world [1–3]. At 25 kV-AC, there are monovoltage systems (1 × 25 kV, with or without the use of booster transformers), and there are bivoltage systems (2 × 25 kV, also called autotransformer-fed systems). This article is about 2 × 25 kV electric railway systems and specifically about the distribution of main currents in these systems.

The 2 × 25 kV electric railway systems are fed by three-winding single-phase transformers, whose primary is connected to the high-voltage transmission system, from an electric utility, and the secondary and the tertiary are at 25 kV (each one), in order to feed the traction system of the electric railway system at 50 kV, with the middle point connected to ground (2 × 25 kV). These windings at 25 kV feed the catenary and the feeder. The catenary system is the group of subconductors that are directly connected to the trains, and the feeder system is a group of subconductors that follow the rail path in order to connect the autotransformers. Furthermore, there are parallel paths for ground currents through rails, ground conductors, and physical earth. The trains are electrically connected to the catenary system through pantographs and to the ground system through rails. The use of autotransformers facilitates the transmission of high magnitudes of power in long distances because there is a main transmission of power at twice of the train voltage (25 kV). The 2 × 25 kV electric railway system is usually applied for high-speed trains because they are typically characterized by long distances and high magnitudes of power.

The distributions of currents in 2×25 kV electric railway systems have been sometimes described in an oversimplified way [4–9], but there are also documents that consider that those distributions of currents are not so simple [10–22]. Some simplified distributions, dependent on train position, are described in [10, 11] without considering the mutual-impedances between the catenary and feeder. A load flow algorithm is described in [12], and the problem related to the distribution of currents among different subconductors of catenary, feeder and ground is solved using a 12×12 line impedance matrix. A simplified load flow algorithm is described in [13], and it is shown that the distribution of currents at both sides of a train is dependent on train position. An approximate monovoltage equivalent model is proposed in [14, 15] in order to simplify the problem related to the bivoltage electrical railway system. A current-based Newton-Raphson power flow algorithm is proposed in [16], and it is compared with other nonlinear solving options. Other options to solve the power flow problem in these systems have also been studied; for example, the use of Thévenin equivalents based on port characteristic equations [17] and the use of an algorithm based on a modified nodal analysis [18]. On the other hand, the 2×25 kV electric railway systems have also been analyzed in order to deal with topics that are not covered in this article; for example, to study the distribution of currents among ground paths [19, 20], solutions dependent on frequency [21] or electromagnetic transients [22] (obviously, these other phenomena are also important, but they are not within the scope of this article).

The catenaries of different railways on the same path have usually been grouped into a single equivalent conductor to facilitate the analysis [3, 4, 6–10, 13–16, 20, 21], as it is considered in this article. On the other hand, the subconductors of the catenary of each railway in the same path can also be grouped to obtain an equivalent conductor for each catenary [11, 17, 18]. These simplifications can be avoided by the solution of the original $N \times N$ line impedance matrix [5, 12, 19, 22], where N is the number of subconductors of the model and it can reach values near to 15 for the simple case of two railways in the same path. The solution of the detailed electric network, considering the original $N \times N$ line impedance matrices, obviously offers a more meticulous system representation, but the option of grouping subconductors in equivalent conductors has been often preferred because facilitates the system solution and the phenomena understanding.

The summary of the literature about this topic shows different options to solve the power flow problem in these systems [10–18]. From those solutions, the calculation of the distribution of currents between catenary and feeder and among autotransformers would be possible, but these details have not been shown in the literature because the goal of these documents has not been the analysis of this point. Thus, the simple question about how the current of one train is distributed through the main paths (equivalent catenary, equivalent feeder, and ground) remains without a simple and proper answer after the review of the literature on this topic. Only some simplistic answers [4–9] were available (without solving the load flow problem), but such simplistic answers are extremely imprecise (e.g., in some references, the train current is multiplied by assumed distribution factors, such as 1/4, 3/4, and/or 1/2, regardless of train position). This article offers a straightforward answer to that question, based on simple analytic equations that are also useful for an approximate solution to the load flow problem. That is, this article shows the way to compute the approximated distribution of the analyzed currents, based only on system impedances and train position, without the need for the accurate solving of the detailed load flow problem.

Only the distribution of main currents in 2×25 kV electric railway systems under normal conditions is covered in this article. The problem related to the distribution of main currents under fault conditions (i.e., short-circuits) is very interesting, but it has to be covered in a future article for the sake of clarity.

This article analyzes the distribution of currents in 2×25 kV electric railway systems under normal conditions. The network equations are clearly formulated, in a way that enables their numerical solution as well as the development of a novel simplified analytical solution. Two analytical deductions for a simplified problem formulation are shown, which are very useful to obtain easy and approximate solutions of the load flow, as well as for a clear understanding about the distribution of currents between catenary and feeder and among autotransformers. On the other hand, the effects of the train position and the autotransformer short-circuit impedances on the distribution of currents are clearly explained, and a similar analysis is not available in the previous literature. These contributions are important for researchers and for professional engineers because: (a) they offer a clear description of the distribution of these currents and (b) offer a simplified solving tool for this problem.

The next sections of this article have been organized in the following way: Section 2 describes the detailed models for the numerical solution of the problem. Section 3 describes the proposed method for the simplified analytical solution, where the autotransformers are considered ideal (i.e., their impedances are null, in contrast with the real autotransformers, whose impedances are not null). Section 4 describes the numerical results, and it is split into two parts: (a) subsection 4.1 shows the results for linear cases with ideal autotransformers, which are identical using the analytical deductions of Section 3 or the numerical solution of Section 2 and (b) subsection 4.2 shows the results for linear and nonlinear cases with real autotransformers, which can only be accurately computed using the numerical solution of Section 2, and are useful to highlight the suitability of the developed analytical method as an approximate solution. Section 5 is devoted to the conclusion.

2. Detailed Models for the Numerical Solution of the Problem

2.1. Brief Description of 2×25 kV Electric Railway Systems. Figure 1 is useful to illustrate an initial description of the 2×25 kV electric railway systems. A cell is defined by the space between autotransformers (or between the three-

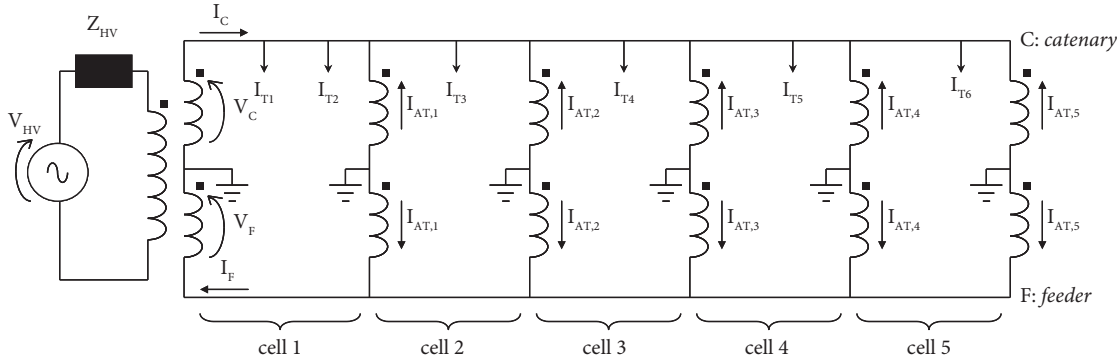

Figure 1: Sketch to illustrate an initial description of 2×25 kV electric railway systems.

winding main transformer and the first autotransformer, in the case of the first cell). The typical distance between autotransformers is around 10 km. The number of autotransformers and trains shown in Figure 1, taken from [14, 15], is higher than usual because it is intended to represent the feeding of some cells from an adjacent substation, (which is not the usual condition but is, herein, covered since it is not an electrical system under fault conditions).

Two or more different railways could be in the same path, and each railway has a catenary (e.g., two catenaries are typically installed for railways in the same path, which are often applied for trains travelling in the opposite direction). In these cases, the catenaries of these different railways are usually connected in parallel at the autotransformer locations (as well as feeders, which are usually connected in parallel at the same locations). Thus, the equivalent catenary and the equivalent feeder of Figure 1 do not represent in detail the catenaries and feeders of each railway in the same path. Despite this fact, simplified schemes (such as the one shown in Figure 1) have been frequently analyzed in the literature about this point [3, 4, 6–10, 13–16].

The turns ratio of autotransformers is 2:1 (both windings of each autotransformer have the same number of turns). The currents in both windings of each autotransformer are identical since the magnetizing currents can be considered negligible. In Figure 1, the currents at autotransformers are $I_{\mathrm{AT}i}$ ($i = 1$ to N_{AT}; N_{AT}: number of autotransformers). For the sake of simplicity, the short-circuit impedances of autotransformers (Z_{AT}) are assumed to be identical for all the autotransformers.

The trains are connected between the catenary and the rails. In Figure 1, the currents at the trains are I_{Tj} ($j = 1$ to N_T; N_T: number of trains). Initially, the trains are considered here as sources of current in order to obtain a linear system. Afterwards, the nonlinear system is solved using a very simple iterative procedure, based on updating the assumed train currents in order to keep the specified values of power.

For each point in the catenary, the current (I_C) is the sum of the currents of the downstream located trains (I_{Tj}) minus the sum of the currents of the downstream located autotransformers ($I_{\mathrm{AT}i}$). On the other hand, for each cell, the current in the feeder (I_F) can be computed as the sum of the currents of the downstream autotransformers ($I_{\mathrm{AT}i}$). Therefore, for each point of the railway path, the sum of the currents of the downstream located trains is $I_C + I_F$.

2.2. Model for Feeders, Catenaries, and Rails. The Carson's line model is usually applied to the geometry of feeders, catenaries, and rails in order to obtain the parameters of a primitive impedance matrix (e.g., a 14×14 matrix [5], or a 12×12 matrix [15]). This primitive impedance matrix can be reduced to a 2×2 system (equivalent catenary C, equivalent feeder F, and reference [15]). Thus, the self-impedances of the 2×2 system are Z_C and Z_F for catenary and feeder, respectively, and Z_{M} is the mutual impedance. The traditional signs for voltages and currents in the line model are shown in Figure 2(a), whereas the convenient signs for feeder variables are shown in Figure 2(b). Thus, the main equations for the line model are as follows:

$$\begin{aligned} \Delta V_C &= V_{C,1} - V_{C,2} = Z_C I_C - Z_M I_F, \\ \Delta V_F &= V_{F,1} - V_{F,2} = Z_M I_C - Z_F I_F. \end{aligned} \tag{1}$$

$V_{C,1}$ and $V_{C,2}$ are the voltages at both line-ends of a catenary segment; $V_{F,1}$ and $V_{F,2}$ are the voltages at both line-ends of a feeder segment; ΔV_C and ΔV_F are the voltage drops in a catenary and a feeder segment, respectively. Herein, the arrow points of voltage correspond to points with the plus sign of the correspondent voltages.

The use of a 2×2 model has been previously applied (e.g., [14, 15]), and it is convenient for the sake of simplicity, but the way of considering the ground currents in this model is not evident. Due to this fact, Appendix A shows a simplified explanation of this point, even though it is not strictly indispensable to understand this article.

2.3. Model for the Three-Winding Transformer. The three-winding transformer is modelled with its conventional equivalent circuit (Figure 3). Due to the polarity shown in Figure 1, special attention must be paid to the signs of I_F and V_F. As the net impedance connected to the primary (Z_{PNET}) is $Z_{\mathrm{HV}} + Z_P$, the main equations for this element can easily include the Thévenin equivalent of the source (Z_{HV} is the impedance of the Thévenin equivalent of the source, and V_{HV} is the correspondent Thévenin voltage)

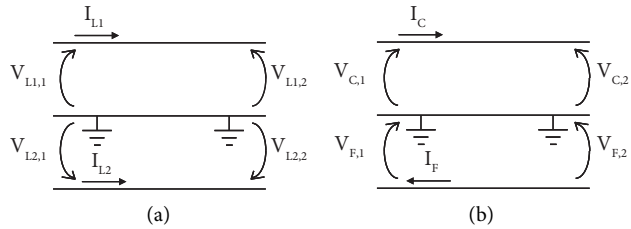

Figure 2: Sketch to illustrate the signs in the line model: (a) traditional line model and (b) required model in accordance with Figure 1.

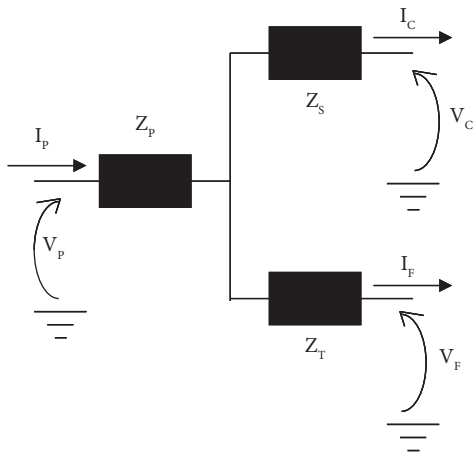

Figure 3: Traditional equivalent model for the 3-winding transformer. Z_P, Z_S, and Z_T are primary, secondary, and tertiary impedances (in pu).

$$V_{HV} = V_C + Z_S I_C + Z_{PNET} I_P,$$
$$V_{HV} = V_F + Z_T I_F + Z_{PNET} I_P. \quad (2)$$

2.4. Model for Autotransformers. The node equations can be easily formulated for catenary and feeder at autotransformer locations. By using the signs in Figure 4, the voltage equation for each autotransformer is as follows:

$$V_{ATF,i} = V_{ATC,i} + Z_{AT} I_{AT,i} \quad (3)$$

$V_{\mathrm{ATC},i}$ and $V_{\mathrm{ATF},i}$ are the voltages at catenary and feeder sides of the autotransformer i, respectively.

2.5. Summary of Linear Equations. Given the source voltage (V_{HV}) and the currents in the trains (I_{Ti}) as known data, the linear problem can be formulated using the autotransformer variables ($I_{\mathrm{AT}i}$, $V_{\mathrm{ATC}i}$, and $V_{\mathrm{ATF}i}$) as main unknowns. Therefore, the number of unknowns is three times the N_{AT}.

For each cell, an equation for the catenary is formulated by expressing the downstream $V_{\mathrm{ATC}j}$ as a function of the upstream $V_{\mathrm{ATC}i}$ (or V_{HV}, in the case of the first cell) and the voltage drops in each subsection of the catenary of this cell. Similarly, for each cell, an equation for the feeder is formulated by expressing downstream $V_{\mathrm{ATF}j}$ as a function of upstream $V_{\mathrm{ATF}i}$ (or V_{HV}, in the case of the first cell) and the voltage drops in each subsection of the feeder of this cell. The key point is that the current at each subsection of catenary is the sum of the currents of the downstream located trains minus the sum of the currents of the downstream autotransformers (Figure 1); on the other hand, the feeder current in each cell is the sum of the currents of the downstream autotransformers (Figure 1). Thus, these equations are mainly based on the mutual- and self-impedances of the afore-described 2×2 matrix, and there are N_{AT} equations for catenary and N_{AT} equations for feeder.

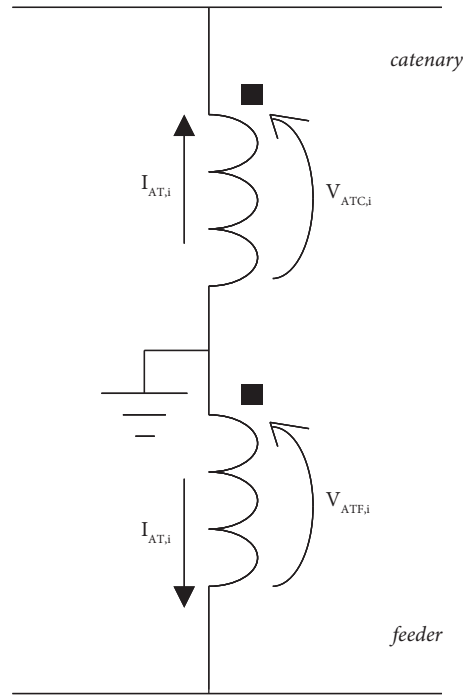

Figure 4: Sketch to illustrate the variables and their signs in autotransformers.

For each autotransformer, the equation (3) relates its variables. Therefore, these N_{AT} equations complete the linear system of $3N_{\mathrm{AT}}$ equations with $3N_{\mathrm{AT}}$ unknowns. Obviously, the system dimension could be reduced using substitution methods, but the $(3N_{\mathrm{AT}}) \times (3N_{\mathrm{AT}})$ system was considered convenient in order to directly obtain the required solution of the main unknowns.

2.6. Nonlinear Solution. Once the linear equations have been properly formulated, the nonlinear problem can be easily formulated by considering that the input data of the trains are the values of power (S_{Tj}) instead of the values of current (I_{Tj}). The nonlinear problem of having power data instead of

current data is traditional in power system analysis, and it has been solved in different ways [23]. The Gauss–Seidel's method [23] was applied in this work, and it is quite simple: (a) the values of train voltages (V_{Tj}) are initially assumed in order to compute the values of train currents ($I_{Tj} = [S_{T_j}/V_{T_j}]^*$) for the first iteration and (b) subsequently, the linear problem is solved, to compute the values of train voltages for the second iteration, and this procedure is repeated until the difference between the computed values of train voltages in two consecutive iterations is lower than the tolerance value (i.e., until the convergence is reached). There are previous works related to the use of nonlinear solving methods [12–18], as well as other methods that could be applied in the future (e.g., forward-backward sweep algorithms), in order to compare different options, but such comparisons are not directly related to the goal of this article. On the other hand, different methods to solve systems of nonlinear equations are currently available as simple software tools (that could be applied if it is considered necessary). The method herein applied is probably the simplest one, and it was considered suitable for the purpose of this article since it was fast and efficient for the analyzed example.

3. Analytical Solution for Simplified Linear Cases with Ideal Autotransformers

For the sake of simplicity, a case with only one train is initially analyzed. In this case, there are three cell types: (a) type-1, where the train is located; (b) type-2, downstream of type-1 cell; and (c) type-3, upstream of type-1 cell.

The autotransformers are considered ideal (i.e., their impedances are null). Thus, $V_{\mathrm{ATC},i} = V_{\mathrm{ATF},i}$ ($i = 1$ to N_{AT}). This condition implies that, for a given cell, the voltage drop at the catenary must be equal to the voltage drop at the feeder. For type-2 cells, this condition is fulfilled because the currents (and voltage drops) at the catenary and feeder are equal to zero.

The first deduction is for type-3 cells (Figure 5). The voltage drop at the catenary (ΔV_C) must be equal to the voltage drop at the feeder (ΔV_F). Therefore,

$$Z_C I_C - Z_M I_F = -Z_M I_C + Z_F I_F \tag{4}$$

Thus,

$$\frac{I_F}{I_C} = \frac{(Z_C + Z_M)}{(Z_F + Z_M)}. \tag{5}$$

This quotient only depends on the line parameters. If the current in the train is known (I_T), another equation can be formulated because $I_C + I_F$ is the sum of the currents of the trains downstream ($I_T = I_F + I_C$). Thus, a linear 2×2 system can be solved in order to obtain I_F and I_C. On the other hand, it is clear that I_F must be different than I_C because Z_C is different than Z_F.

The second deduction is for type-1 cells (Figure 6). $I_{C,i}$ is the current through the subsection of catenary between the train and the adjacent autotransformer nearest to the source. As the currents at both windings of autotransformers must

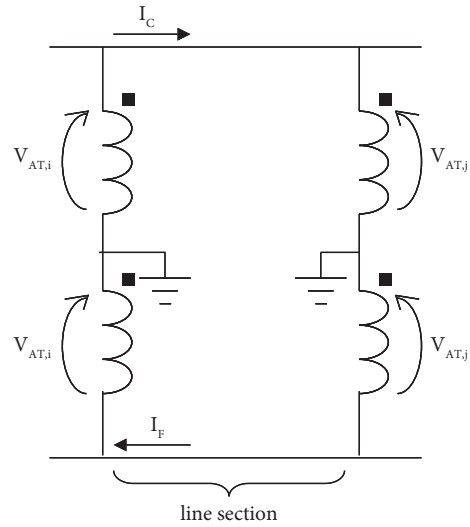

Figure 5: Sketch to illustrate the deduction for type-3 cells.

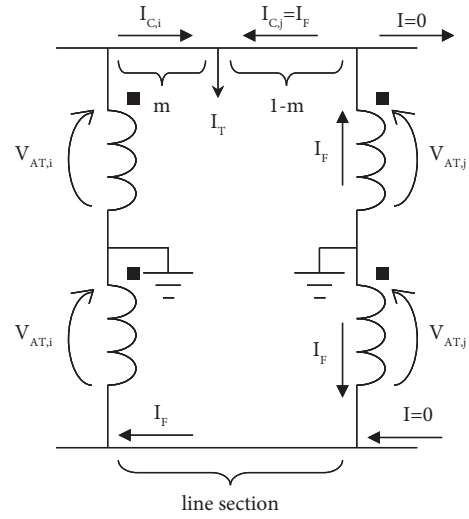

Figure 6: Sketch to illustrate the deduction for type-1 cell.

be equal to each other, and the downstream currents must be null, the current in the other subsection of the catenary ($I_{C,j}$) must be equal to I_F. Again, ΔV_C must be equal to ΔV_F; therefore,

$$\begin{aligned} &mZ_C I_{C,i} - \left((1-m)Z_C I_F + Z_M I_F\right) \\ &\quad = -mZ_M I_{C,i} + \left((1-m)Z_M I_F + Z_F I_F\right). \end{aligned} \tag{6}$$

Thus,

$$\frac{I_F}{I_{C,i}} = \frac{I_{C,j}}{I_{C,i}} = \frac{(m(Z_C + Z_M))}{(Z_F + (2-m)Z_M + (1-m)Z_C)}. \tag{7}$$

This quotient depends on the line parameters and m (where m is the distance up to the train, in per unit of the line length for this cell, measured from the adjacent autotransformer, which is nearest to the source). Again, if the current in the train is known ($I_T = I_{C,i} + I_{C,j} = I_{C,i} + I_F$), a linear 2×2 system can be easily solved to obtain I_F and $I_{C,i}$.

For the first cell, a convenient simplification is the assumption that $Z_S = Z_T = 0$ for the 3-winding transformer. Thus, the first cell can be considered as type-1 or type-3, depending on whether the train is in this cell or not.

The case of multiple trains can be solved by superposition. That is, N_T cases (N_T: number of trains) with only one train can be independently solved in order to superpose the obtained currents. An advantage of this procedure is that the solution is directly found by simple analytical equations. For example, this feature was useful for debugging the numerical solving algorithm described in Section 2. On the other hand, the deductions for the cases with multiple trains could also be obtained (similar to the deductions described for cases with only one train); however, the number of variables is greater, and the solution is not so simple as in the case of only one train.

4. Numerical Results

The numerical method described in Section 2, considering multiple trains and real autotransformers, was successfully verified with the help of the solution shown in [15]. The numerical results for this article are obtained using the system illustrated in Figure 1, whose main data were taken from [15] and are included in Appendix B. These numerical results are split into two subsections: (4.1) linear cases with ideal autotransformers and (4.2) linear and nonlinear cases with real autotransformers. The results of subsection 4.1 are identical when using the analytical deductions of Section 3 or the numerical solution of Section 2. The results of subsection 4.2 can only be accurately computed using the numerical solution of Section 2 and are useful to show the suitability of the developed analytical method as an approximate solution. Finally, subsection 4.3 is devoted to offering a summarized analysis of results related to the purpose of this article.

4.1. Results for Linear Cases with Ideal Autotransformers

4.1.1. Distribution of Currents for Cases with Only One Train. In this example, only I_{T5} is not null for the system shown in Figure 1, and this train is located at the cell midpoint. $I_{T5} = 1\ \text{pu}/\underline{-10^\circ}$, $V_{\text{HV}} = 1\ \text{pu}/\underline{0^\circ}$, and $Z_P = Z_S = Z_T = 0$. This case was analytically solved through the deductions in Section 3 and also numerically solved through the algorithm in Section 2. The numerical differences between the results are extremely low (i.e., insignificant). The main results are shown in Figure 7. These results are important for understanding the distribution of currents.

For the sake of clarity, the step-by-step description of the analytical solution is shown here. Step a: the current at the catenary and the current at the feeder in cell 5 are both zero because it is a type-2 cell. Step b: the cell 4 is a type-1 cell, and the quotient $I_F/I_{C,i} = 0.25/4^\circ$ is obtained by substitution of data (Appendix B) in equation (7) with $m = 0.5$. Step c: the current at catenary and the current at feeder in cell 4 are obtained by the solution of $I_F/I_{C,i} = 0.25/4^\circ$, and $I_{C,i} + I_F = 1\ \text{pu}/-10^\circ$. Step d: the cells 1, 2, and 3 are type-3 cells, and the quotient $I_F/I_C = 0.69/5^\circ$ is obtained by substitution of data (Appendix B) in equation (5). Step e: the current at the catenary and the current at the feeder in cells 1, 2, and 3 are obtained by the solution of $I_F/I_C = 0.69/5^\circ$ and $I_C + I_F = 1\ \text{pu}/-10^\circ$.

The main results are the currents in the autotransformers because the other currents can be obtained from them. In this case, only I_{AT3} and I_{AT4} are not null in the autotransformers. Visually, the autotransformers in Figure 7 seem to be in parallel, but they are not in parallel. The key point is that the voltage drops in the catenary and feeder must be equal to each other (line model) if the autotransformers are considered ideal. Consequently, the afore-described "Step e" shows that the currents in the catenary for all the type-3 cells must be equal to each other, as well as the currents in the feeder for all the type-3 cells must be equal to each other (therefore, $I_{\text{AT1}} = I_{\text{AT2}} = 0$).

As shown in (5) and (7), these distributions of currents are dependent on mutual- and self-impedances of the 2×2 line impedance matrix. Actually, I_C and I_F are constant in cells 1, 2, and 3 of this example because the line impedances were assumed to be homogeneous. If the line impedance matrix of one of these cells were different than the line impedance matrix of an adjacent cell (which can occur due to some maintenance needs), then I_C and I_F could be different for those adjacent cells; consequently, the difference of the currents would circulate by autotransformers 1 and/or 2 in that case.

At each point of the railway path, the current in the catenary must be the sum of the current in the feeder plus the current through the ground paths (rails, ground conductors, and physical earth). That is, for cells 1, 2, and 3, the current through the ground path is not null (and this point has been sometimes oversimplified [3–9]). The equation (5) clearly shows that I_F is equal to I_C only if Z_C is equal to Z_F (i.e., for type-3 cells, the current by the ground path can only be null if Z_C is equal to Z_F).

On the other hand, if the train position is varied from $m = 0$ to 1, the main distributions of currents are shown in Figure 8. The current through the subsection of catenary between the train and the adjacent autotransformer nearest to the source ($I_{C,3}$) is equal to the train current for $m = 0$, and it is minimum ($0.59 I_{T5}$) for $m = 1$. $I_{C,4}/I_{C,3}$ is the graphical result of equation (7) for this example, and it indicates the ratio for currents at both sides of the catenary for the cell where the train is located. $I_{\text{AT},3}/I_{T5}$ and $I_{\text{AT},4}/I_{T5}$ indicate how much of the train current circulates by the nearest autotransformers.

4.1.2. Distribution of Currents for a Case with Multiple Trains. In this example: $I_{T1} = 1\ \text{pu}/\underline{-10^\circ}$, $I_{T2} = 1\ \text{pu}/\underline{-10^\circ}$, $I_{T3} = 1\ \text{pu}/\underline{-15^\circ}$, $I_{T4} = 1\ \text{pu}/\underline{-15^\circ}$, $I_{T5} = 1\ \text{pu}/\underline{-20^\circ}$, $I_{T6} = 1\ \text{pu}/\underline{-20^\circ}$. These trains are located at $m = 0.001$, 0.9, 0.8, 0.7, 0.6, and 0.5, respectively, and $V_{\text{HV}} = 1\ \text{pu}/\underline{0^\circ}$ and $Z_P = Z_S = Z_T = 0$. This case was analytically solved using the deductions from Section 3 for only one train and the superposition method to obtain the sum of currents in each autotransformer. Furthermore, this case was also numerically solved using the algorithm of Section 2 (and considering simultaneously the six trains). The numerical differences in the results are insignificant. The main results are shown in Table 1. The

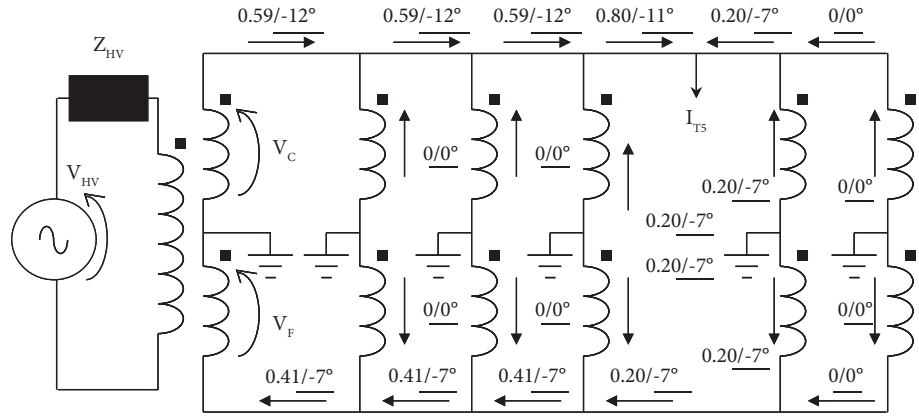

Figure 7: Currents for the example with only one train, with $Z_{AT} = 0\%$ and the train located at the cell midpoint.

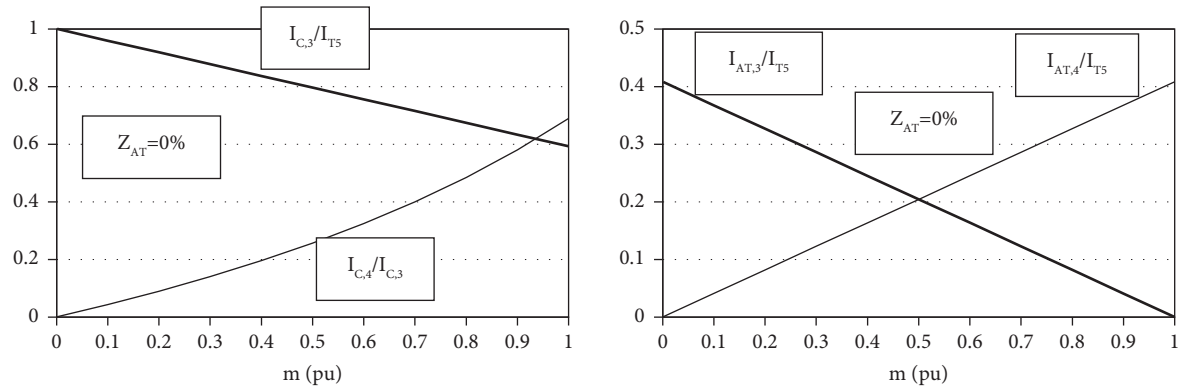

Figure 8: Main distributions of currents as a function of train position (m) for the example with only one train and ideal autotransformers.

Table 1: Autotransformer currents (in pu) for the example with six trains and ideal autotransformers.

Case	I_{AT1}	I_{AT2}	I_{AT3}	I_{AT4}	I_{AT5}
Only T1	<0.01	0	0	0	0
Only T2	$0.37\angle -7^\circ$	0	0	0	0
Only T3	$0.08\angle -12^\circ$	$0.33\angle -12^\circ$	0	0	0
Only T4	0	$0.13\angle -12^\circ$	$0.29\angle -12^\circ$	0	0
Only T5	0	0	$0.16\angle -17^\circ$	$0.25\angle -17^\circ$	0
Only T6	0	0	0	$0.20\angle -17^\circ$	$0.20\angle -17^\circ$
6 trains	$0.45\angle -8^\circ$	$0.45\angle -12^\circ$	$0.45\angle -14^\circ$	$0.45\angle -17^\circ$	$0.20\angle -17^\circ$

current in autotransformer 1, in the case of only T1, is very low because this train is located very near the 3-winding transformer. On the other hand, the current in autotransformer 5 for the case with only T6 is exactly equal to the correspondent result for the case of six trains (because only this train contributes to the current in this autotransformer). Conceptually, the superposition method is useful to see that the currents in autotransformers are mainly due to trains located at cells on both sides of the autotransformers.

4.2. Results for Linear and Nonlinear Cases with Real Autotransformers

4.2.1. Results for Linear Cases with Real Autotransformers. In this section, the autotransformer impedances (Z_{AT}) are included in the simulation; therefore, the results only can be numerically obtained. That is, the results of this section are not predictable with accuracy using analytical equations, unlike the results of the previous section. For example, in cases with only one train, the currents are not mathematically equal to zero for those autotransformers which are not at each end of the cell with the train. The results are herein shown as a function of Z_{AT} in order to show the influence of Z_{AT} on the distribution of currents. In practice, Z_{AT} tends to be very low (nearly 1%). The highest considered value of Z_{AT} (5%), however, is much higher than the typical values in real life. The resistive part of Z_{AT} was assumed to be 0.5% in all these examples.

Table 2 shows the main results for examples similar to the previous example with only one train, but Z_{AT} is not zero in these cases. That is, $I_{T5} = 1\ \text{pu}\angle -10^\circ$, the train is located at the cell midpoint ($m = 0.5$), and $V_{HV} = 1\ \text{pu}\angle 0^\circ$, for the results shown in Table 2. On the other hand, Figure 9 shows the

Table 2: Autotransformer currents (in pu) for the example with only one train and real autotransformers.

Z_{AT} (%)	I_{AT1}	I_{AT2}	I_{AT3}	I_{AT4}	I_{AT5}
1.0	<0.01	0.02/−14°	0.19/−6°	0.19/−6°	0.02/−15°
1.5	<0.01	0.02/−6°	0.18/−7°	0.18/−7°	0.02/−6°
2.0	<0.01	0.03/−3°	0.17/−8°	0.17/−8°	0.03/−3°
3.0	<0.01	0.03/−2°	0.16/−9°	0.16/−9°	0.04/−0.4°
4.0	<0.01	0.04/−2°	0.15/−10°	0.16/−9°	0.05/0.1o
5.0	0.01/5°	0.04/−2°	0.15/−10°	0.15/−10°	0.05/−0.1o

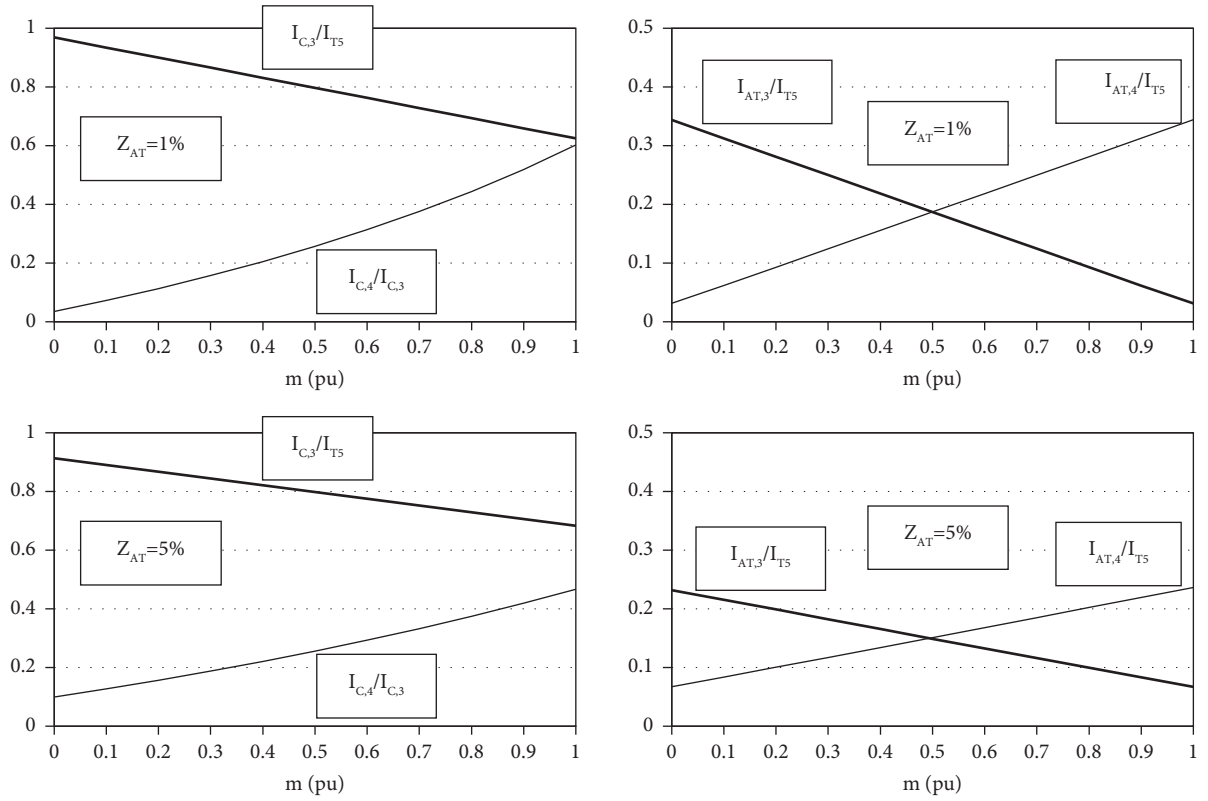

Figure 9: Main distributions of currents as a function of train position (m) for the example with only one train and real autotransformers.

main distributions of the currents as a function of the train position (m) for the example with $I_{T5} = 1\,\text{pu}/\underline{-10^\circ}$, $V_{HV} = 1\,\text{pu}/\underline{0^\circ}$, and real autotransformers ($Z_{AT} \neq 0$). The results for $Z_{AT} = 1\%$ are very similar to those of the ideal case, and the differences are amplified as the value of Z_{AT} is greater.

Table 3 shows the distribution of currents for examples similar to the previous example with multiple trains, but Z_{AT} is not zero in these cases. The train currents and train locations are exactly the same as in the previous example with multiple trains. Again, these results show that the case of $Z_{AT} = 1\%$ gives results similar to the ideal case, and the differences are amplified as the value of Z_{AT} is greater.

Figure 10 shows the distribution of currents for the example of six trains with $Z_{AT} = 1\%$ (which is a typical value for these autotransformers). Results for the case with $Z_{AT} = 0\%$ are also shown, between parenthesis, for comparison purposes. It is clear that differences in results are not significant, and this point can be complemented by the fact that the currents in trains are permanently changing.

On the other hand, results for the example of six trains with $Z_{AT} = 1\%$ were numerically obtained using the algorithm of Section 2, whereas results with $Z_{AT} = 0\%$ can be analytically obtained using the deductions of Section 3. Thus, it is clear that the analytical deductions of Section 3 are useful to obtain an approximate solution to the distribution of currents in these systems.

4.2.2. Results for the Nonlinear Case. Table 4 shows the distribution of currents for examples similar to the ones shown in Table 3, but the input data are the values of the power in each train instead of the current. For the sake of similarity with the previous case, the input data of power were chosen equal to the previous data of current, changing the angle sign (that is, considering that the voltage at the trains is relatively near to $1\,\text{pu}/\underline{0^\circ}$). The input data for power are: $S_{T1} = S_{T2} = 1\,\text{pu}/\underline{10^\circ}$, $S_{T3} = S_{T4} = 1\,\text{pu}/\underline{15^\circ}$, $S_{T5} = S_{T6} = 1\,\text{pu}/\underline{20^\circ}$. The remaining conditions for the simulations are exactly the same as the previous example. The maximum differences

Table 3: Autotransformer currents (in pu) for the example with six trains and real autotransformers.

Z_{AT} (%)	I_{AT1}	I_{AT2}	I_{AT3}	I_{AT4}	I_{AT5}
1.0	$0.41\angle -8^\circ$	$0.45\angle -12^\circ$	$0.45\angle -14^\circ$	$0.43\angle -16^\circ$	$0.23\angle -18^\circ$
1.5	$0.39\angle -9^\circ$	$0.44\angle -12^\circ$	$0.44\angle -14^\circ$	$0.42\angle -17^\circ$	$0.23\angle -17^\circ$
2.0	$0.38\angle -9^\circ$	$0.44\angle -12^\circ$	$0.44\angle -14^\circ$	$0.42\angle -17^\circ$	$0.24\angle -15^\circ$
3.0	$0.36\angle -11^\circ$	$0.43\angle -13^\circ$	$0.44\angle -14^\circ$	$0.41\angle -17^\circ$	$0.25\angle -15^\circ$
4.0	$0.34\angle -12^\circ$	$0.42\angle -13^\circ$	$0.43\angle -15^\circ$	$0.40\angle -17^\circ$	$0.26\angle -15^\circ$
5.0	$0.32\angle -13^\circ$	$0.41\angle -14^\circ$	$0.43\angle -15^\circ$	$0.40\angle -17^\circ$	$0.27\angle -15^\circ$

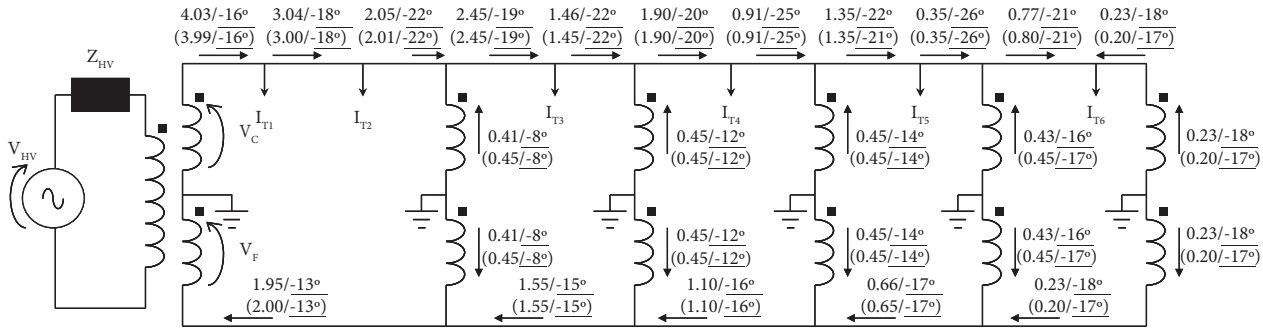

Figure 10: Distribution of currents for the example with six trains (results with $Z_{AT} = 1\%$ are shown without parenthesis, whereas results with $Z_{AT} = 0\%$ are shown between parenthesis).

Table 4: Autotransformer currents (in pu) for the example with six trains and the nonlinear method. First example.

Z_{AT} (%)	I_{AT1}	I_{AT2}	I_{AT3}	I_{AT4}	I_{AT5}
1.0	$0.43\angle -10^\circ$	$0.48\angle -16^\circ$	$0.49\angle -19^\circ$	$0.48\angle -22^\circ$	$0.25\angle -24^\circ$
1.5	$0.41\angle -11^\circ$	$0.47\angle -16^\circ$	$0.49\angle -19^\circ$	$0.47\angle -23^\circ$	$0.26\angle -23^\circ$
2.0	$0.40\angle -12^\circ$	$0.47\angle -16^\circ$	$0.49\angle -20^\circ$	$0.46\angle -23^\circ$	$0.27\angle -23^\circ$
3.0	$0.38\angle -14^\circ$	$0.46\angle -17^\circ$	$0.48\angle -20^\circ$	$0.45\angle -23^\circ$	$0.28\angle -22^\circ$
4.0	$0.36\angle -15^\circ$	$0.45\angle -18^\circ$	$0.47\angle -20^\circ$	$0.45\angle -23^\circ$	$0.29\angle -21^\circ$
5.0	$0.34\angle -16^\circ$	$0.44\angle -18^\circ$	$0.47\angle -21^\circ$	$0.44\angle -23^\circ$	$0.30\angle -21^\circ$

Table 5: Autotransformer currents (in pu) for the example with six trains and the nonlinear method. Second example.

Z_{AT} (%)	I_{AT1}	I_{AT2}	I_{AT3}	I_{AT4}	I_{AT5}
1.0	$0.40\angle -5^\circ$	$0.45\angle -11^\circ$	$0.46\angle -14^\circ$	$0.45\angle -18^\circ$	$0.24\angle -19^\circ$
1.5	$0.39\angle -6^\circ$	$0.45\angle -11^\circ$	$0.46\angle -14^\circ$	$0.44\angle -18^\circ$	$0.24\angle -18^\circ$
2.0	$0.38\angle -7^\circ$	$0.44\angle -11^\circ$	$0.45\angle -15^\circ$	$0.43\angle -18^\circ$	$0.25\angle -18^\circ$
3.0	$0.36\angle -9^\circ$	$0.44\angle -12^\circ$	$0.45\angle -15^\circ$	$0.42\angle -18^\circ$	$0.26\angle -17^\circ$
4.0	$0.34\angle -10^\circ$	$0.43\angle -13^\circ$	$0.44\angle -15^\circ$	$0.42\angle -18^\circ$	$0.27\angle -16^\circ$
5.0	$0.32\angle -11^\circ$	$0.42\angle -13^\circ$	$0.44\angle -16^\circ$	$0.41\angle -18^\circ$	$0.28\angle -16^\circ$

between the results of the currents in Tables 3 and 4 are 12%, and such differences are mainly due to the fact that the voltage is 1 pu$\angle 0^\circ$ at the source, not at the trains. Again, these differences in the results are not significant, especially considering that the currents in the trains are permanently changing (due to the behaviour of drivers and/or the locations of trains). In order to approximate the effect of voltage drops, a difference of 0.05 pu in the magnitudes and 5° in the angles was included in the input data. The input data of power for this second example are $S_{T1} = S_{T2} = 0.95\ \text{pu}\angle 5^\circ$, $S_{T3} = S_{T4} = 0.95\ \text{pu}\angle 10^\circ$, and $S_{T5} = S_{T6} = 0.95\ \text{pu}\angle 15^\circ$, and the results are shown in Table 5. The maximum differences between the results of the currents in Tables 3 and 4 are 4%. Obviously, the differences in the results could be greater if the voltages in the trains are not near 1 pu. This condition is not typical at all, but it is possible since these systems are often designed to operate with minimum voltages near 0.69 pu (therefore, the nonlinear method should be the preferred option in those atypical conditions).

4.3. Summarized Analysis of Results Related to the Purpose of This Article. The results with ideal autotransformers, as shown in Table 1, were obtained through two independent methods (the analytical solution shown in Section 3 and the linear numerical solution explained in Section 2). Both methods are alternative ways of obtaining the accurate solution in the case of ideal autotransformers. The analytical method can be easily implemented by the simple writing of formulas of Section 3 in a worksheet, whereas the linear numerical solution explained in Section 2 can be easily obtained by coding the correspondent program.

The autotransformer impedances are very low in practice (nearly 1%). Under these circumstances, the distribution of current among autotransformers, and between catenary and feeder in the case of real transformers is similar to the corresponding results in the case of ideal autotransformers. This fact can be easily verified by the comparison of results with $Z_{AT} = 0\%$ and with $Z_{AT} = 1\%$ in the following places: (a) Figure 7 and Table 2; (b) Tables 1 and 3; (c) Figures 8 and 9; and (d) Figure 10. Therefore, the results with ideal autotransformers offer an approximate solution to the distribution of currents in the case of real autotransformers.

The results of linear and nonlinear methods are similar to each other if the train voltages are near to 1 pu. This fact can be easily verified by comparing the results of Table 3 with those of Tables 4 or 5 (differences in these results are

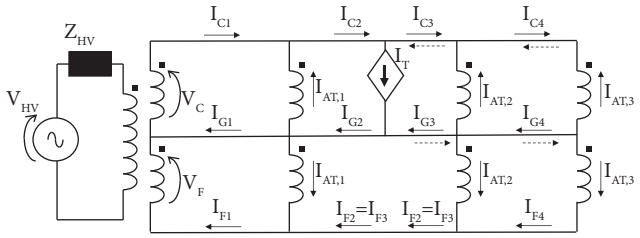

Figure 11: Sketch to illustrate the circulation of ground currents (I_{Gk}) in the 2×2 line model for 2×25 kV electric railway systems. Arrows with solid lines are according to the sign convention of this article, and arrows with dashed lines indicate that the usual result is in the opposite direction.

unimportant, especially considering that the currents in the trains are permanently changing).

The distribution of currents in these systems can be clearly understood with the help of (a) Figure 7, whose results are based on equations (5) and (7) of Section 3, and (b) Table 1 and the values between parenthesis in Figure 10, whose results are based on Section 3 and the superposition method.

5. Conclusion

The distribution of currents in 2×25 kV electric railway systems under normal conditions was herein analyzed in detail. The network equations were clearly described, and this description enabled their numerical solution as well as the formulation of an analytical solution for simplified cases. The transformer impedances were initially neglected in order to obtain the required simplification for the approximate analytical solution. This analytical tool facilitates the explanation of the distribution of currents among autotransformers and between catenary and feeder, as well as the effect of train position on the distribution of these currents. Afterwards, the autotransformer short-circuit impedances were included in order to show their effect on the distribution of computed currents.

The distribution of currents among autotransformers is simple because currents circulate mainly through autotransformers located on both sides of one train. The superposition method is useful to explain the distribution of currents in cases with multiple trains.

The distribution of currents between catenary and feeder for the cells located upstream of the trains is mainly defined by the differences among the impedances of the line 2×2 model. The distribution of currents between catenary and feeder for the cells with trains is mainly defined by the train location and by the impedances of the line 2×2 model. Obviously, the autotransformer impedances have an effect on the results, but this effect is not significant for the typical values of autotransformer impedances (around 1%).

The trains can be modelled as constant current or constant power. The differences in results can be considered negligible if the voltages in the trains are near to 1 pu, which is the usual condition. On the other hand, if the voltages in the trains are not near to 1 pu (which is possible, under some unusual conditions) and the trains need to be modelled as constant power, the nonlinear method should be applied in order to properly compute the currents in the electrical system. In general, modelling trains as having a constant current can be a convenient simplification, especially considering that the currents in trains are constantly changing.

Nomenclature

I_{ATi}:	Currents at autotransformers are I_{ATi} ($i = 1$ to N_{AT}; N_{AT}: number of autotransformers)
Z_{AT}:	Short-circuit impedances of autotransformers (Z_{AT})
I_{Tj}:	Currents at trains ($j = 1$ to N_T; N_T: number of trains)
Z_{HV}:	Impedance of the Thévenin equivalent of the source, at the connection point for the three-winding transformer
V_{HV}:	Thévenin voltage of the equivalent source at the connection point for the three-winding transformer
I_C:	Current in the catenary
I_F:	Current in the feeder
Z_C, Z_F:	Self-impedances of the 2×2 system for catenary and feeder, respectively
Z_M:	Mutual impedance between catenary and feeder of the 2×2 system
$V_{C,1}$, $V_{C,2}$:	Voltages at both ends of a catenary segment
$V_{F,1}$, $V_{F,2}$:	Voltages at both ends of a feeder segment
ΔV_C:	Voltage drop in a catenary segment
ΔV_F:	Voltage drop in a feeder segment
I_{L1}, I_{L2}:	Currents in the traditional line model
$V_{L1,1}$, $V_{L2,1}$, $V_{L1,2}$, $V_{L2,2}$:	Voltages in the traditional line model
Z_{PNET}:	Net impedance connected to the primary of the three-winding transformer
Z_P, Z_S, Z_T:	Primary, secondary, and tertiary impedances of the three-winding transformer
$V_{ATC,i}$, $V_{ATF,i}$:	Voltage at catenary and feeder sides of the autotransformer i
S_{Ti}:	Complex power in train j
V_{Tj}:	Voltage at train j
$I_{C,i}$:	Current through the subsection of catenary between the train and the adjacent autotransformer nearest to the source
$I_{C,j}$:	Current through the subsection of catenary between the train and the adjacent autotransformer most far from the source
m:	Distance up to the train, from the adjacent autotransformer nearest to the source, in per unit of the line length of the cell
I_{Gk}:	Net ground current in section k.

Appendix

A. Ground Currents in the 2 × 2 Model Feeders, Catenaries, and Rails

The analysis of models for lines with multiple phase conductors and multiple ground conductors is well-known in the case of three-phase systems; this point was clearly understood many years ago to develop the electrical power systems. For example, a classical textbook [24] shows a proper way to perform the matrix reductions to group the multiple subconductors of phase and ground, as well as to take off the ground conductors from the line model formulation. That is, the primitive matrix has all the details of all the subconductors and the earth effect, and the result is a 3 × 3 reduced model of the three-phase transmission lines (phases a, b, and c; without specific terms for ground elements). It is well-known that the 3 × 3 line model of three-phase transmission lines considers that ground currents are the sum of phase currents, and the self- and mutual-impedances of ground conductors have been included in such a reduced model. Similarly, in the 2 × 2 model of Figure 2, the ground current is simply $I_{L1} + I_{L2}$ (Figure 2(a)) or $I_C - I_F$ (Figure 2(b)), and this ground current is the sum of the currents flowing through all the ground paths. Figure 11 illustrates the distribution of currents in an example with only 3 cells, for the sake of simplicity; the currents at each point of the catenary and feeder (I_{Ck} and I_{Fk}) can be directly obtained using the 2 × 2 model, and the net ground current (I_{Gk}) can be easily computed as $I_{Gk} = I_{Ck} - I_{Fk}$ at each point.

It is evident that: (a) I_{F4}=$I_{AT,3}$, $I_{C4} = -I_{AT,3}$, $I_{G4} = -2I_{AT,3}$; (b) I_{F3}=$I_{AT,2} + I_{AT,3}$, $I_{C3} = -(I_{AT,2} + I_{AT,3})$, $I_{G3} = -2(I_{AT,2} + I_{AT,3})$. Thus,

$$\begin{aligned} I_{C2} &= I_{C3} + I_T = I_T - \left(I_{AT,2} + I_{AT,3}\right), \\ I_{G2} &= I_{G3} + I_T = I_T - 2\left(I_{AT,2} + I_{AT,3}\right), \\ I_{C1} &= I_{C2} - I_{AT,1} = I_T - \left(I_{AT,1} + I_{AT,2} + I_{AT,3}\right), \\ I_{F1} &= I_{F2} + I_{AT,1} = I_{AT,1} + I_{AT,2} + I_{AT,3}, \\ I_{G1} &= I_{C1} - I_{F1} = I_T - 2\left(I_{AT,1} + I_{AT,2} + I_{AT,3}\right). \end{aligned} \tag{A.1}$$

For this particular case, the application of Section 3 of this article implies that: (a) the currents in cell 3 tend to be negligible ($I_{AT,3} \approx 0$); consequently, $I_{G4} \approx 0$; (b) the ratio between the currents in catenary and feeder (I_F/I_C) in cell 1 is dependent on self- and mutual-impedances of the 2 × 2 line model; consequently, I_{G1} is in general different than zero.

B. Data of the System Taken as an Example [15]

Equivalent source (utility): $Z_{HV} = 0$.

3-winding transformer ($S_{BASE} = 80$ MVA; $V_{BASE\text{-}LV} = 27.5$ kV): $Z_P = j0.075$ pu; $Z_S = j0.025$ pu; $Z_T = j0.025$ pu

Line (2 × 2 matrix for the catenary/feeder system):

$$Z_C = (0.81091 + j2.3755).10^{-3} \text{ pu/km}$$
$$Z_F = (1.78320 + j3.8437).10^{-3} \text{ pu/km}$$
$$Z_M = (0.33677 + j1.2436).10^{-3} \text{ pu/km}$$

Each autotransformer ($S_{BASE} = 10$ MVA; $V_{BASE\text{-}LV} = 27.5$ kV): $Z_{AT} = 0$ or $j0.05$ pu in [15], whereas Z_{AT} (in %) = 0, 1, 1.5, 2, 3, 4, or 5 in this article (with a resistive part equal to 0.5%).

Distance between autotransformers: 10 km.

Data Availability

The data used to support the findings of this study are included within the article.

Conflicts of Interest

The authors declare that they have no conflicts of interest

Acknowledgments

Elmer Sorrentino is grateful to Erick Oliveros (GE, UK), José Antonio Sandoval (ABB, Spain), Nilda Sánchez (Network Rail, UK), Daniel Díaz (Instituto de Ferrocarriles del Estado, Venezuela, R.I.P.), and Stefano Lauria (Universitá di Roma, Italy) for their valuable help.

References

[1] D. Serrano-Jiménez, L. Abrahamsson, S. Castaño-Solís, and J. Sanz-Feito, "Electrical railway power supply systems: current situation and future trends," *International Journal of Electrical Power & Energy Systems*, vol. 92, pp. 181–192, 2017.

[2] F. Kiessling, R. Puschmann, A. Schmieder, and E. Schneider, *Contact Lines for Electrical Railways: Planning - Design - Implementation*publicis, Paris, France, 2009.

[3] F. Schmid and C. Goodman, "Electric railway systems in common use," in *Proceedings of the 4th IET Professional Development Course on Railway Electrification Infrastructure and Systems*, p. 15, London, UK, June 2009.

[4] M. Plakhova, B. Mohamed, and P. Arboleya, "Static model of a 2×25kV AC traction system," in *Proceedings of the 6th International Conference on Power Electronics Systems and Applications*, pp. 1–5, Hong Kong, China, December 2015.

[5] L. Battistelli, M. Pagano, and D. Proto, "2$\,\times\,$25-kV 50 Hz high-speed traction power system: short-circuit modeling," *IEEE Transactions on Power Delivery*, vol. 26, no. 3, pp. 1459–1466, July 2011.

[6] T. Ho, Y. Chi, J. Wang, K. Leung, L. Siu, and C. Tse, "Probabilistic load flow in AC electrified railways," *IEE Proceedings - Electric Power Applications*, vol. 152, no. 4, pp. 1003–1013, July 2005.

[7] Areva T&D Ibérica S. A., "Protecciones de Aistancia. Guía de aplicación, Cap. 13: Sistemas Ferroviarios 1x25kV y 2x25kV," (in Spanish), 2005.

[8] Areva T&D, "Network Protection & Automation Guide (Chapter 20: Protection of A.C. Electrified Railways)," 2002.

[9] R. Hill and I. Cevik, "On-line simulation of voltage regulation in autotransformer-fed AC electric railroad traction networks," *IEEE Transactions on Vehicular Technology*, vol. 42, no. 3, pp. 365–372, 1993.

[10] B. Mohamed, P. Arboleya, and M. Plakhova, "Current injection based power flow algorithm for bilevel 2x25kV railway systems," in *Proceedings of the 2016 Power and Energy Society General Meeting*, pp. 1–5, Boston, MA, USA, July 2016.

[11] A. Capasso, N. Ciaccio, R. Lamedica, A. Prudenzi, and B. Perniceni, "Un modello semplificato per il calcolo elettrico

dei sistemi di trazione ferroviaria 2x25 kv - 50 hz," *Ingegneria Ferroviaria*, pp. 529–538, 1995.

[12] S. Li, "Power flow in railway electrification power system," Master Thesis, New Jersey Institute of Technology, New Jersey, NJ, USA, 2010.

[13] S. Raygani, A. Tahavorgar, S. Fazel, and B. Moaveni, "Load flow analysis and future development study for an AC electric railway," *IET Electrical Systems in Transportation*, vol. 2, no. 3, pp. 139–147, Sept. 2012.

[14] E. Pilo, L. Rouco, A. Fernández, and L. Abrahamsson, "A monovoltage equivalent model of bi-voltage autotransformer-based electrical systems in railways," *IEEE Transactions on Power Delivery*, vol. 27, no. 2, pp. 699–708, April 2012.

[15] E. Pilo, *Diseño óptimo de la electrificación de ferrocarriles de alta velocidad (in Spanish)*, PhD Thesis, Universidad Pontificia Comillas de Madrid, Spain, 2003.

[16] K. Mongkoldee and T. Kulworawanichpong, "Current-based Newton-Raphson power flow calculation for AT-fed railway power supply systems," *International Journal of Electrical Power & Energy Systems*, vol. 98, pp. 11–22, June 2018.

[17] J. Zhang, M. Wu, and Q. Liu, "A novel power flow algorithm for traction power supply systems based on the Thévenin equivalent," *Energies*, vol. 11, no. 1, pp. 126–217, Jan. 2018.

[18] B. Mohamed, P. Arboleya, I. El-Sayed, and C. Gonzalez-Moran, "High-speed 2×25 kV traction system model and solver for extensive network simulations," *IEEE Transactions on Power Systems*, vol. 34, no. 5, pp. 3837–3847, Sep, 2019.

[19] S. Minucci, M. Pagano, and D. Proto, "Model of the 2×25kV high speed railway supply system taking into account the soil-air interface," *International Journal of Electrical Power & Energy Systems*, vol. 95, pp. 644–652, Feb. 2018.

[20] M. Ceraolo, "Modeling and simulation of AC railway electric supply lines including ground return," *IEEE Transactions on Transportation Electrification*, vol. 4, no. 1, pp. 202–210, March 2018.

[21] A. Mariscotti, P. Pozzobon, and M. Vanti, "Simplified modeling of 2$\,\times\,$25-kV at railway system for the solution of low frequency and large-scale problems," *IEEE Transactions on Power Delivery*, vol. 22, no. 1, pp. 296–301, Jan. 2007.

[22] B. Milesevic, B. Filipovic-Grcic, I. Uglesic, and B. Jurisic, "Estimation of current distribution in the electric railway system in the EMTP-RV," *Electric Power Systems Research*, vol. 162, pp. 83–88, Sep. 2018.

[23] F. Milano, *Power System Modelling and Scripting*, Springer, Berlin, Germany, 2010.

[24] P. Anderson, *Analysis of Faulted Power Systems*, IEEE Press, Piscataway, NJ, USA, 1995.